ELSEVIER

Journal of Power Sources 91 (2000) 143–149

JOURNAL OF POWER SOURCES

www.elsevier.com/locate/jpowsour

Oxidation of electrodeposited lead–tin alloys in 5 M H_2SO_4

I. Petersson, E. Ahlberg *

Department of Chemistry, Göteborg University, SE-41296 Gothenborg, Sweden

Received 8 March 1999; received in revised form 23 February 2000; accepted 23 February 2000

Abstract

By electroplating lead–tin alloys on a lightweight substrate material, such as glassy carbon, it is possible to obtain less dense electrodes with good contact between the active material and the substrate. The former is especially important for the lead–acid battery since it has relatively low energy density compared to many other battery systems. In order to obtain higher power densities for applications in, for example, electric or hybrid vehicles, the weight of the battery needs to be minimised.

In the present investigation, the oxidation of electrodeposited lead–tin alloys in 5 M H_2SO_4 was studied as a function of tin concentration. The alloys were prepared by electrodeposition and the oxidation behaviour was studied by the means of cyclic voltammetry. Microstructural information on the deposited layer was obtained by scanning electron microscopy (SEM).

The experimental results show that electrodeposited lead–tin alloys contain a supersaturated solid solution phase with up to 12 at.% Sn. Oxidation of this phase in 5 M H_2SO_4 leads to the formation of a PbO phase with increased conductivity compared to pure PbO. In addition, the amounts of PbO and PbO_2 decrease with increasing amounts of tin in the alloy and for high tin alloys, where a bulk tin phase is present, no PbO phase is observed.

Keywords: Lead–tin alloys; PbO reduction; Oxidation; Lead–acid battery; Cyclic voltammetry

1. Introduction

In lead–acid batteries, lead–tin (Pb–Sn) alloys have been used to overcome the passivation problems following the replacement of the traditional Pb–Sb grids with antimony-free or low antimony alloys [1]. Passivation of lead and lead alloys is believed to occur by the formation of highly resistive α-PbO at the interface between the grid and the active material during the oxidation of lead to lead dioxide, passivating the electrical contact over the boundary layer [2–7]. α-PbO is formed under the lead sulphate layer where the local pH value is close to 9 due to the semi-permeable properties of the lead sulphate layer, allowing a flux of H^+, OH^- and water species, while hindering SO_4^{2-} and HSO_4^- ions [7]. A solution to this problem has been to add tin as an alloying element to lead. Studies indicate that alloying with tin makes the PbO layer thinner [8,9], promotes the oxidation of tet-PbO or α-PbO to PbO_n ($1 < n < 2$), and lowers the potential at which this reaction initiates [10,11]. Two comprehensive reviews covering the literature about the role of tin as an alloying element to eliminate problems of passivation have been presented by Nelson and Wisdom [12] and by Culpin et al. [13]. Thus, the presence of tin in the oxide layer has been confirmed, but its chemical composition and oxidation state of tin are still debated.

Hämeenoja et al. [14] studied the mechanism of oxide growth on Pb, Pb–Ca alloy and Pb–Ca–Sn alloy and low-Sb alloys in H_2SO_4. The growth of these oxide layers was found to follow a parabolic rate law indicating that the rate of the oxide layer growth is diffusion controlled. Further, it was shown that the oxidation rate for the alloys was higher than that of pure lead at 200 mV [14]. The increase in the oxidation rate was explained by either an increase in the number of oxygen vacancies caused by the introduction of cations with a lower valence than IV in the lead dioxide layer, or by an increase in the electronic conductivity, i.e., an introduction of cations with a higher valence than (II) in the layer. Using photoelectrochemical techniques, Pavlov et al. [11] proposed a mechanism for the tin-catalysed oxidation of α-PbO to PbO_n ($1 < n < 2$) by means of the incorporation of Sn^{3+} in the lead oxide crystal lattice. The incorporated tin ions caused an increase in the hole concentration, and thereby, an increased con-

* Corresponding author. Tel.: +46-31-772-2879; fax: +46-31-772-2853.

E-mail address: ela@inoc.chalmers.se (E. Ahlberg).

0378-7753/00/$ - see front matter
PII: S0378-7753(00)00459-6

ductivity, which in turn caused an increase in reaction rate [11]. Döring et al. [10] also assumed an increase in the conductivity of the passivating layer via the formation of a mixed semi-conducting Pb–Sn oxide. By a combination of photoelectrochemistry, electrochemical impedance and rotating ring disk measurements, Bojinov et al. [15] found that tin facilitated the oxidation of Pb^{2+} to Pb^{4+} by 0.1–0.2 V. They also found that addition of tin both stabilised and increased the amount of non-stoichiometric oxide. Salmi and Sundholm [18] showed by means of ring–disk measurements that tin dissolves from the alloy as Sn^{2+}, both in the active dissolution and in the passive region, whereas Sn^{4+} ions do not appear at potentials lower than 3 V. They also found that an addition of Sn^{2+} ions to the solution seemed to inhibit the formation of PbO_2. This was in agreement with the work carried out by Ijomah [16,17]. Salmi and Sundholm [18] suggested that either a semi-conducting Pb–Sn oxide or a highly tin-doped PbO_n oxide is formed on the alloyed material. Using electrochemical techniques and XPS, numerous investigations of the electrical properties of the passivation layer in both alkaline and acid solutions were presented [19–25]. The main conclusion from these investigations was that a significant increase in the conductivity of the oxide was observed at a tin content larger than 1 wt.% followed by a plateau at 2.5 wt.%. Various explanations to the observed properties have been suggested such as a percolation mechanism with conducting tin oxide. The decrease observed in conductivity for long periods of time was explained by the slow dissolution of tin oxide in sulphuric acid [24]. A disproportionation mechanism between PbO and SnO has also been suggested but no certain evidence of the formed phases was presented [26]. Also, Sn(IV) oxide has been used to explain the increased conductivity of PbO precipitated at the grain boundaries [27].

In the present investigation, the oxidation of electrodeposited lead–tin alloys in 5 M H_2SO_4 was studied as a function of tin concentration. The alloys were prepared by electrodeposition from a 1 M HBF_4 solution and the oxidation behaviour was studied by the means of cyclic voltammetry. Microstructural information of the deposited layer was obtained by scanning electron microscopy (SEM). The results show that both the amounts of PbO_2 and PbO decreased with increasing amount of tin in the alloy. In addition, the peak corresponding to the reduction of PbO moved in the positive direction with increasing tin content in the alloy, indicating an increased conductivity of this phase.

2. Experimental

2.1. Reagents and electrochemical cell

All the electrochemical experiments were performed in a conventional three-electrode cell with the possibility of using a rotating disk electrode. The electrolyte solution was bubbled with purified nitrogen for at least 30 min prior to the experiment and this atmosphere was kept constant during the experiment. All potentials are referred to a double-junction Ag/AgCl electrode, $E = 197$ mV with respect to SHE. The inner compartment was filled with a solution saturated with KCl and AgCl, and the outer compartment contained 1 M HBF_4 or 5 M H_2SO_4 depending on the experimental conditions. The working electrode consisted of a glassy carbon disk, $\varnothing = 3$ mm, moulded in epoxy, with only one side exposed to the electrolyte. Before the experiments, the surface was wet-ground with silicon carbide paper (1000 and 4000 mesh) and rinsed, first in ethanol in an ultrasonic bath and then in distilled water, after which the electrode was immediately transferred to the electrochemical cell. A platinum gauze was used as auxiliary electrode and the potential was controlled by an EG&G Princeton Applied Research potentiostat/galvanostat Model 273A. All experiments were carried out at room temperature. To prepare the electrolyte solutions, different amounts of PbO and SnO (p.a., Merck) were added to 1 M HBF_4. The 1 M HBF_4 solution was prepared from 50 wt.% HBF_4 (purum, Merck). In the tin-containing solutions, pure granulated tin (p.a., Merck) was added to avoid oxidation of Sn(II) during the experiments. The 5 M H_2SO_4 solution was prepared from 18 M H_2SO_4 (p.a., Merck).

2.2. Electroplating

Working electrodes for the oxidation study were prepared by electrodeposition of lead, tin and lead–tin alloys on the pre-treated glassy carbon electrode described in Section 2.1. The deposits were electroplated from a 1 M HBF_4 solution containing various concentrations of the metals to be alloyed. In this process, the electrode was conditioned for 60 s at 0 V before the potential was stepped to the deposition potential, -550 mV, where it was held for 300 s. After the deposition process, the electrode was rinsed in distilled water and immediately placed in the 5 M H_2SO_4 solution. This process and the characterisation of these electrodes have been described in detail in a previous work by the authors [28].

2.3. Cyclic voltammetry

Cyclic voltammetry sweeps for oxidation of Pb–Sn alloys in 5 M H_2SO_4 were recorded as a function of increasing tin ion concentration in a 0.01 M Pb solution. In addition to pure lead and tin, the tin concentrations examined were 0.5, 1, 1.5, 2, 5, 10, 20, 50, 77 and 90 mol%. Three different potential ranges were investigated. In the first range, the potential scan was initiated at -0.7 V swept in the positive direction to 0 V, where the potential was reversed to a final value of -0.7 V. The next cycle was initiated at the same potential but reversed first at 2.1

V, followed by −0.7 V, and ending at 1.0 V. In the final potential range, the cyclic voltammogram was obtained by initiating the potential scan at −0.7 V and scanning in the positive direction until the potential was reversed at 2.1 V and finally ended at −0.9 V.

2.4. Differential pulse anodic stripping voltammetry — DPASV

According to this method, the metal or the alloy is first deposited on a GC disk and subsequently anodically dissolved in the same electrolyte. The electrode is conditioned for 60 s at 0 V before the potential is stepped to −550 mV, unless stated otherwise, and the deposition time is 20 s. The scan rate during stripping was 1 mV s^{-1} and the differential pulse voltammograms were recorded as a function of increasing tin ion concentration in a 0.01 M Pb solution. The experimental data were evaluated by a peak deconvolution program (Peak Solve, Galactic), where the amount of charge for each current peak was determined by integration of the area under the peak after being fitted to a log-normal function.

2.5. Scanning electron microscopy — SEM

The samples used in the SEM study were electrodeposited on the electrode, removed from the electrolyte and rinsed with distilled water and acetone before identification. Before transfer to the microscope, the samples were covered with carbon. The morphology of the different electrodeposits was characterised by a scanning electron microscope (JEOL JSM-5300).

3. Results and discussion

3.1. Oxidation

In Fig. 1, voltammograms for electrodeposited lead and tin are compared. In 5 M H_2SO_4, lead is oxidised at more

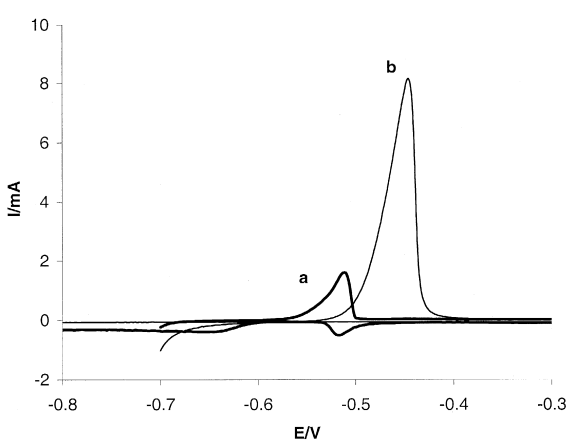

Fig. 1. Voltammetric characteristics of electrodeposited (a) Pb and (b) Sn in 5 M H_2SO_4. Sweep rate: 20 mV s^{-1}.

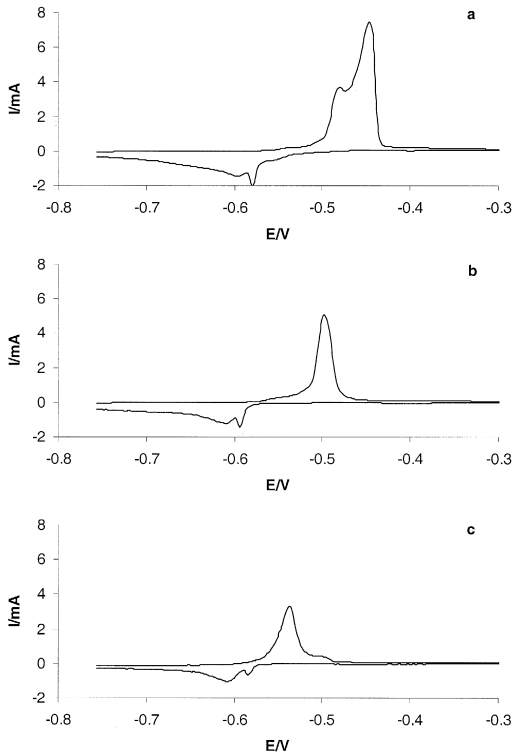

Fig. 2. Voltammetric characteristics of electrodeposited Pb–Sn alloys in 5 M H_2SO_4: (a) 80 at.% Sn, (b) 50 at.% Sn and (c) 10 at.% Sn. Sweep rate: 20 mV s^{-1}.

negative potentials compared to tin, forming insoluble lead sulphate on the surface, which prevents further oxidation. In the first cycle, no oxidation of lead sulphate is observed up to a potential of 2.1 V where oxygen starts to evolve. On the negative-going scan, a peak appears at −0.52 V corresponding to the reduction of PbO, formed underneath the passive layer of lead sulphate. At slightly more negative potentials, lead sulphate is reduced to lead metal. From the appearance of the voltammetric peak this process seems to be controlled by diffusion. The electroreduction of $PbSO_4$ has been relatively little studied [29] and more recently, two different explanations to the diffusion limiting process have been forwarded. Varela et al. [30,31] showed by use of cyclic voltammetry and potentiostatic current transients that an instantaneous nucleation and 3D-growth mechanism under diffusion control could describe the process. In addition, the cause of diffusion control has been attributed to Pb^{2+} formed by dissolution of $PbSO_4$ [32,33]. In contrast to this, the electroreduction of PbO was shown to obey a progressive nucleation and 3D-growth mechanism under charge transfer control [34].

One large oxidation peak is observed for tin. Since the solubility of tin sulphate is high compared to lead sulphate, all of the electrodeposited metal is dissolved during the first scan. Hence, the back scan only demonstrates the characteristics of the glassy carbon substrate.

The influence of lead on the characteristics of tin is shown in Fig. 2. The sweeps are initiated in the positive

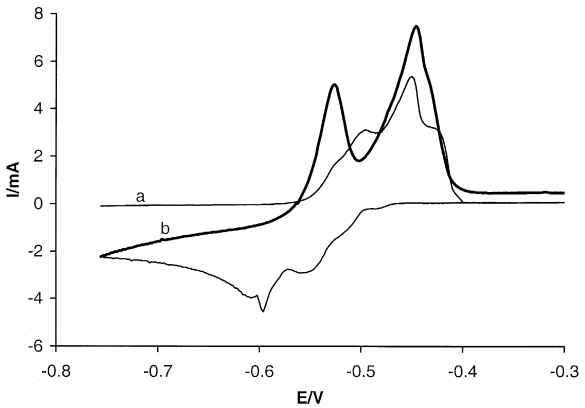

Fig. 3. Repetitive cyclic voltammetry for a Pb–Sn alloy containing 80 at.% Sn, showing the change in the alloy composition on cycling. (a) Second cycle and (b) third cycle. The first cycle is shown in Fig. 2a.

going direction with a switching potential of 0 V, which is well below further oxidation of the passive layer. For a composition of 1 mM Pb^{2+} + 10 mM Sn^{2+}, corresponding to 20 at.% lead in the alloy [28], two anodic peaks are observed (Fig. 2a). The second peak corresponds to the dissolution of pure tin, while the first peak appears at more positive potentials than pure lead (Fig. 1). The first peak is therefore attributed to the dissolution of a Pb–Sn phase. Most of the tin is oxidised to form soluble species, but some are trapped under the passive layer and transforms into tin oxide. When the lead content in the alloy is increased, the formation of lead sulphate prevents dissolution of tin. On the back scan, two peaks are observed, one small and sharp peak corresponding to the reduction of tin oxide underneath the passivating layer and one broad peak for the reduction of lead sulphate. By increasing the concentration of lead to 50 at.% in the alloy (2.6 mM Pb^{2+} + 10 mM Sn^{2+}), only one oxidation peak is observed, at a potential between the oxidation peaks for the pure metals (Fig. 2b). Even though lead and tin are deposited side by side the interaction is so strong that the Pb–Sn phase behaves like a homogeneous phase exhibiting intermediate oxidation properties. On the back scan, the peak corresponding to the reduction of tin oxide decreases at the expense of the lead sulphate reduction. Further increase of the lead content results again in two anodic peaks (Fig. 2c). The first peak corresponds to the oxidation of pure lead, while the small peak at slightly more positive potentials shows the dissolution of the Pb–Sn phase. On the back scan, the reduction peak for tin oxide is further decreased.

3.2. Decomposition of the Pb–Sn phase

The oxidation–reduction cycle shown in Fig. 2 causes a change in the composition of the alloy. Tin dissolves from the surface layer, while lead is reformed on the negative going sweep by the reduction of lead sulphate. Since a stationary electrode is used, some of the dissolved tin ions will be reduced as well. On the second cycle, which proceeds to 2.1 V, a more complex voltammogram is therefore seen, with a separation of the oxidation and reduction peaks in several contributions, as illustrated in Fig. 3. On the subsequent sweep, two peaks corresponding to the dissolution of the pure metals appear.

3.3. Microstructure of lead–tin alloys

In Fig. 4, the microstructure of the electrodeposited Pb–Sn alloys is shown by backscatter images. For the alloy containing 20 at.% lead, only small particles of pure lead (white dots with a diameter of ~ 0.5 μm) are noticed. A close look at the voltammogram (Fig. 2a) indeed shows a small peak for dissolution of bulk lead at about -0.53 V. However, the main peak is divided into two, corresponding to dissolution of bulk tin and a Pb–Sn phase. In the latter case, lead sulphate is formed as a solid oxidation product. However, at this low lead concentration in the alloy, only partial passivation of the surface takes place and the dissolution of tin is readily observed. When the alloy contains equal amounts of tin and lead, a structure with alternating layers of tin (grey) and lead (white) is observed (Fig. 4b). The voltammogram in this case shows only one oxidation peak on the first cycle (Fig. 2b). Lead

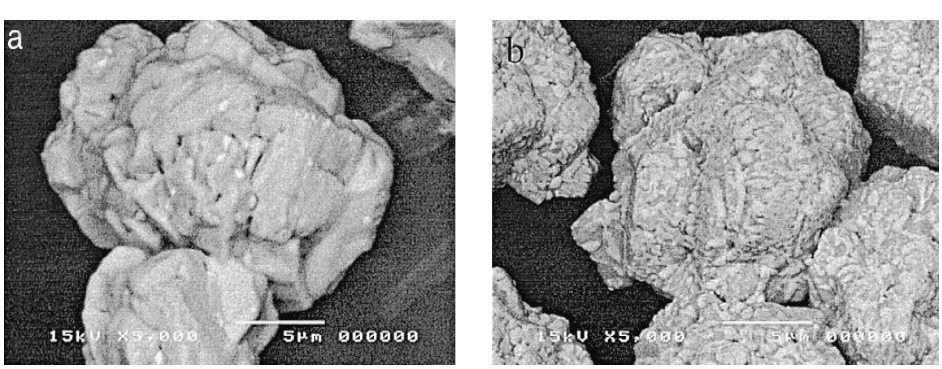

Fig. 4. SEM backscatter images for Pb–Sn alloys deposited from a solution containing (a) 1 mM Pb^{2+} + 10 mM Sn^{2+} and (b) 2.6 mM Pb^{2+} + 10 mM Sn^{2+}, respectively. The white part consists of the lead phase.

is oxidised forming lead sulphate, which by its large molar volume occupies the total surface area and thus prevents oxidation of tin in the alloy. This is evident from the subsequent cycles, where bulk lead is accumulated on the surface, leaving a depleted tin phase that can be dissolved. Finally, for the low tin alloy, the oxidation of bulk lead dominates. However, also in this case, the dissolution of a Pb–Sn phase is clearly observed by the small peak at −0.5 V. Upon cycling this alloy only small change in the voltammetric response is observed, since the dissolution of bulk lead dominates the picture; the peak corresponding to the dissolution of the Pb–Sn phase disappears.

It is quite obvious that the lead dissolution is hindered in the layered structure, which can be explained by interactions between the two separate phases in the alloy, as has been illustrated previously for deposition on glassy carbon [28] and gold [35]. Another possible explanation is that tin and lead form a solid solution. The phase diagram for the Pb–Sn system is well documented [36]. The solubility of lead in tin is very low at room temperature, while the solubility of tin in lead amounts to 3.3 at.% at room temperature. In electrodeposition, it is quite common to observe metastable phases [37] and a supersaturated solid solution has been reported for the Pb–Sn system containing a minimum of 11.3 at.% Sn [38].

3.4. Composition of lead–tin alloys

Anodic stripping voltammetry in 1 M HBF_4 was used to estimate the composition of the electrodeposited alloy. For low concentrations of tin in solution, no distinct peak for tin dissolution can be observed. However, compared to pure lead, a potential shift in the negative direction is observed together with a broadening of the peak. By assuming that these effects originate from the formation of a solid solution of tin in lead, the tin content can be calculated. In Fig. 5, the atomic percent of tin in the alloy is plotted as a function of the molar fraction of tin ions in the solution. The graph shows that the amount of tin in the alloy increases immediately and becomes approximately constant amounting to about 12 at.%. Not until the concentrations of lead and tin in solution become equal, the content of tin in the alloy starts to rise. At these concentrations it is also possible to observe two different peaks in the stripping voltammogram [28]. It is interesting to note that the constant level of 12 at.% Sn at low-bulk concentrations of tin is close to that reported earlier for electrodeposited Pb–Sn alloys [38]. It is therefore reasonable to believe that a solid solution phase is formed.

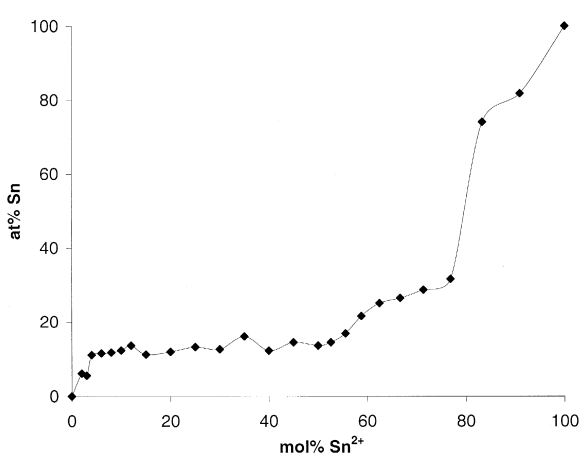

Fig. 5. Atomic percent tin in the alloy as a function of molar fraction tin in the plating solution.

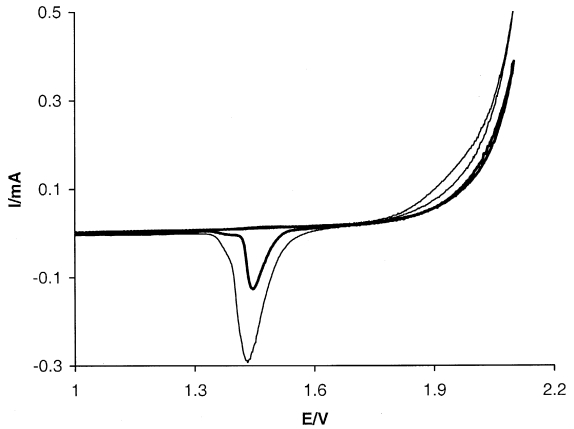

Fig. 6. Cyclic voltammograms (10th cycle) in the potential range of PbO_2 formation, Pb (fine) and Pb12 at.% Sn (bold). Sweep rate: 20 mV s^{-1}.

A qualitative evidence for the formation of a new phase is the fact that the adherence of the deposited layer to the glassy carbon substrate is largely improved in the presence of minute amounts of tin in solution.

3.5. PbO_2 formation

As discussed above, the oxidation of lead sulphate to lead dioxide is not observed on the first scan, since it takes place in parallel with the oxygen evolution. However, by cycling in a potential range from 0 to 2.1 V, a lead dioxide layer is accumulated and a reduction peak for PbO_2 evolves (Fig. 6). Two effects can clearly be observed as the tin concentration increases. Firstly, the amount of PbO_2 decreases drastically and secondly, the overpotential for oxygen evolution increases. Both effects have been observed earlier and were attributed to the formation of a PbO_n phase [18,22].

3.6. Reduction of PbO

Tin in the alloy is believed to increase the conductivity of the PbO phase formed underneath the semi-permeable lead sulphate layer. In Fig. 7, the influence of tin on the reduction of PbO is shown. A cyclic voltammogram is run starting at −0.8 V and proceeding in the positive direction up to 2.1 V, where oxygen evolution starts in parallel with the oxidation of lead sulphate. On the back scan, the

reduction of PbO first appears (shown in Fig. 7) and at more negative potentials lead sulphate is reduced. The reduction of PbO is facilitated by the presence of tin in the alloy, as evident from the positive potential shift. However, as the tin content in the alloy increases, the reduction peak diminishes and the peak potential becomes constant. For higher concentrations of tin, the reduction peak of PbO disappears totally. In Fig. 8, the peak potential for the reduction of PbO is plotted as a function of the concentration of tin in solution. The sharp change in peak potential observed for the lowest concentrations of tin can be attributed to an increasing tin content in the alloy. The fact that the potential reaches a constant value can be understood by comparing with the composition of the alloy determined by anodic stripping voltammetry (Fig. 5). In a large range of concentrations, the amount of tin in the alloy is constant. As the tin content of the alloy increases the formation of PbO is completely hindered and a new peak evolves at more positive potentials. This latter peak was also found for a casted alloy with 10 wt.% tin under similar conditions [18] and was attributed to the reduction of soluble tin species.

The positive shift in potential can be discussed in terms of increasing conductivity of the PbO phase formed. Numerous investigations, both in acid and alkaline environments, have reported an increase in the conductivity of PbO with increasing tin content in the alloy [1,11,15,18, 21,23,24,39–41]. The increased conductivity is due to the formation of a semi-conducting PbO_n phase, which leads to diminishing amounts of PbO_2. This sets a limit for the optimum concentration of tin in the alloy; high enough concentration to prevent the formation of an insulating PbO phase at the grid interface, but low enough to avoid hindrance of PbO_2 formation. It has been stated that the tin content should be between 1 and 2.5 wt.% for optimum performance of the battery These concentrations are very low and fall within the range of solid solution of tin in lead. In the present investigation, where electrodeposited alloys were studied, much higher solid solution concentrations are formed but, anyhow, the performance of these alloys shows the desired effects.

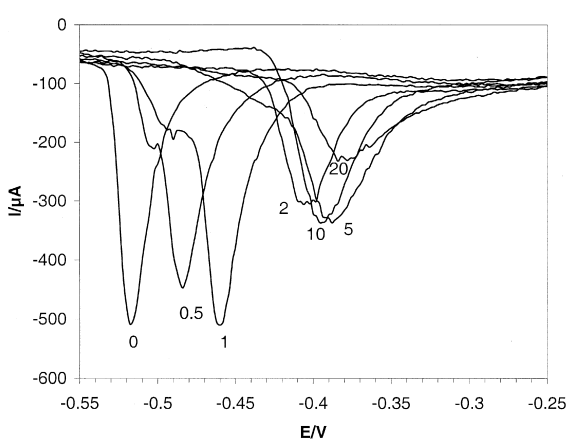

Fig. 7. Voltammograms showing the influence of alloying tin on the reduction of PbO. The numbers refer to mole percent (mol%) of Sn in the plating solution. Sweep rate: 20 mV s^{-1}.

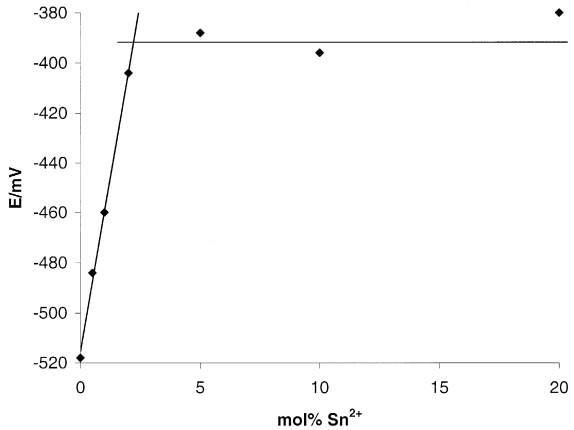

Fig. 8. Peak potential as a function of tin concentration in the plating solution.

By electrodepositing lead–tin alloys on a lightweight substrate material, such as glassy carbon, it is possible to obtain less dense electrodes with good contact between the active material and the substrate. This is especially interesting for applications in electrical or hybrid vehicles where the weight of the battery needs to be minimised in order to obtain high power density for short discharge periods. Bipolar constructions of the lead–acid battery system have been found to be well suited for such applications. However, if the lead–acid battery is to be an attractive candidate in future electric or hybrid vehicles, its relatively low energy density must be significantly increased. A solution to this problem is to minimise its weight.

4. Conclusions

- Electrodeposited lead–tin alloys contain a supersaturated solid solution phase with up to 12 at.% Sn. Oxidation of this phase in 5 M H_2SO_4 leads to the formation of a PbO phase with increased conductivity compared to pure PbO. This is evidenced from the fact that the peak corresponding to the reduction of PbO moves in the positive direction as a function of increasing tin content in the alloy. In addition, the amount of PbO decreases with increasing amounts of tin in the alloy and for high tin alloys, where a bulk tin phase is present, no PbO phase is observed.
- In the presence of tin in the alloy, the oxygen evolution is somewhat hindered and the amount of PbO_2 formed by cycling in 5 M H_2SO_4 decreases with increasing amount of tin in the alloy.

• From the results obtained in the present study, electrodeposited lead–tin alloys seems to be good candidates for use in lightweight lead–acid batteries. A thin layer of the alloy can be deposited on an inert construction material to ensure good contact between the active material and the grid.

Acknowledgements

This work has received financial support from the Swedish National Board for Industrial and Technical Development (NUTEK). The authors wish to thank Lars Eklund for performing the SEM pictures.

References

[1] N. Bui, P. Mattesco, P. Simon, N. Pébère, J. Power Sources 73 (1998) 30.
[2] K.R. Bullock, M.A. Butler, J. Electrochem. Soc. 133 (1986) 1085.
[3] D. Pavlov, R. Popova, Electrochim. Acta 15 (1970) 1843.
[4] J.S. Buchanan, N.P. Freestone, L.M. Peter, J. Electroanal. Chem. 182 (1985) 383.
[5] J.S. Buchanan, L.M. Peter, Electrochim. Acta 33 (1988) 127.
[6] D. Pavlov, C.N. Poulieff, E. Klanja, N. Iordanov, J. Electrochem. Soc. 116 (1969) 316.
[7] P. Ruetschi, J. Electrochem. Soc. 120 (1973) 331.
[8] R. Miraglio, L. Albert, A.E. Ghachcham, J. Steinmetz, J.P. Hilger, J. Power Sources 53 (1995) 53.
[9] K. Giess, in: K.P. Bullock, D. Pavlov (Eds.), Adv. Lead–Acid Batteries 82-14 The Electrochemical Society, Pennington, NJ, USA, 1984, p. 241.
[10] H. Döring, J. Garche, H. Dietz, K. Wiesener, J. Power Sources 30 (1990) 41.
[11] D. Pavlov, B. Monakhov, M. Maja, N. Penazzi, J. Electrochem. Soc. 136 (1989) 27.
[12] R.F. Nelson, D.M. Wisdom, J. Power Sources 33 (1991) 165.
[13] B. Culpin, A.F. Hollenkamp, D.A.J. Rand, J. Power Sources 38 (1992) 63.
[14] E. Hämeenoja, T. Laitinen, G. Sundholm, A. Yli-Pentti, Electrochim. Acta 34 (1989) 233.
[15] M. Bojinov, K. Salmi, G. Sundholm, Electrochim. Acta 39 (1994) 719.
[16] M.N.C. Ijomah, J. Appl. Electrochem. 18 (1988) 142.
[17] M.N.C. Ijomah, J. Electrochem. Soc. 134 (1987) 2960.
[18] K. Salmi, G. Sundholm, J. Power Sources 40 (1992) 217.
[19] P. Simon, N. Buiand, F. Dabosi, J. Power Sources 50 (1994) 141.
[20] P. Simon, N. Bui, N. Pebereand, F. Dabosi, J. Power Sources 53 (1995) 163.
[21] P. Simon, N. Bui, N. Pebere, F. Dabosiand, L. Albert, J. Power Sources 55 (1995) 63.
[22] N. Bui, P. Mattesco, P. Simon, J. Steinmetz, E. Rocca, J. Power Sources 67 (1997) 61.
[23] P. Mattesco, N. Bui, P. Simon, L. Albert, J. Electrochem. Soc. 144 (1997) 443.
[24] P. Mattesco, N. Bui, P. Simon, L. Albert, J. Power Sources 64 (1997) 21.
[25] P. Mattesco, N. Bui, P. Simon, Mater. Sci. Forum 289–292 (1998) 1073.
[26] M. Terada, S. Saito, T. Hayakawa, A. Komaki, Prog. Batteries Sol. Cells 8 (1989) 214.
[27] A.E.G. Amrani, P. Steyer, J. Steinmetz, P. Delacroix, G.L. Caër, J. Power Sources 64 (1997) 35.
[28] I. Petersson, E. Ahlberg, J. Electroanal. Chem., in press.
[29] N.A. Hampson, J.B. Lakeman, J. Power Sources 6 (1981) 101.
[30] F.E. Varela, L.M. Gassa, J.R. Vilche, Electrochim. Acta 37 (1992) 1119.
[31] F.E. Varela, L.M. Gassa, J.R. Vilche, J. Appl. Electrochem. 25 (1995) 358.
[32] P. Ekdunge, K.V. Rybalka, D. Simonsson, Electrochim. Acta 32 (1987) 659.
[33] K. Kanamura, Z. Takehara, J. Electrochem. Soc. 139 (1992) 345.
[34] F.E. Varela, L.M. Gassa, J.R. Vilche, J. Appl. Electrochem. 25 (1995) 364.
[35] I. Petersson, E. Ahlberg, J. Electroanal. Chem., in press.
[36] M. Hansen, Constitution of Binary Alloys, McGraw-Hill, New York, 1958.
[37] A.R. Despic, V.D. Jovic, Mod. Aspects Electrochem. 27 (1995) 143.
[38] Y.N. Sadana, Z.H. Zhang, Surf. Coat. Technol. 34 (1988) 109.
[39] I. Mukhopadhyay, M. Sharon, P. Veluchamy, H. Minoura, J. Electroanal. Chem. 401 (1996) 139.
[40] M. Bojinov, K. Salmi, G. Sundholm, J. Electroanal. Chem. 358 (1993) 177.
[41] M. Bojinov, K. Salmi, G. Sundholm, J. Electroanal. Chem. 347 (1993) 207.